

Alkaline anion exchange membrane fuel cells for cogeneration of electricity and valuable chemicals

Z.F. Pan^a, R. Chen^{b,c}, L. An^{a*}, Y.S. Li^{d*}

^a Department of Mechanical Engineering, The Hong Kong Polytechnic University, Hung Hom, Kowloon, Hong Kong SAR, China.

^b Key Laboratory of Low-grade Energy Utilization Technologies and Systems (Chongqing University), Ministry of Education, Chongqing 400030, China.

^c Institute of Engineering Thermophysics, Chongqing University, Chongqing 400030, China.

^d Key Laboratory of Thermo-Fluid Science and Engineering of MOE, School of Energy and Power Engineering, Xi'an Jiaotong University, 28 Xianning West Road, Xi'an, Shaanxi 710049, China.

*Corresponding authors.

^a E-mail: liang.an@polyu.edu.hk (L. An)

^d E-mail: ysli@mail.xjtu.edu.cn (Y.S. Li)

Abstract

Alkaline anion exchange membrane fuel cells (AAEMFCs) have received ever-increasing attentions due to the enhanced electrochemical kinetics and the

absence of precious metal electrocatalysts, and thus great progress has been made in recent years. The alkaline anion exchange membrane based direct alcohol fuel cells, one type of alkaline anion exchange membrane fuel cells utilizing liquid alcohols as fuel that can be obtained from renewable biomass feedstocks, is another attractive point due to its ability to provide electricity with cogeneration of valuable chemicals. Significant development has been made to improve the selectivity towards high added-value chemicals and power output in the past few years. This review article provides a general description of this emerging technology, including fuel-cell setup and potential reaction routes, summarizes the products, performance, and system designs, as well as introduces the application of this concept in the removal of heavy-metal ions from the industrial wastewater. In addition, the remaining challenges and perspectives are also highlighted.

Keywords: Alkaline anion exchange membrane fuel cells; electrocatalysts; valuable chemicals; power output; system design; removal of heavy-metal ions

1. Introduction

As the energy shortage issues and greenhouse gas effects are increasingly serious, fuel cells that are alternative options for power supply sources have attracted worldwide research interest due to its potential to alleviate the two challenges simultaneously [1, 2, 3, 4, 5, 6]. Fuel cells are one of the most promising clean and efficient energy production technologies that directly convert chemical energy stored in fuels to electricity and heat [7, 8]. Generally, fuel cells can be classified into five types according to the electrolyte employed: alkaline fuel cells (AFCs), polymer electrolyte fuel cells (PEFCs), phosphoric acid fuel cells (PAFCs), molten carbonate fuel cells (MCFCs), and solid oxide fuel cells (SOFCs) [9]. Among them, PEFCs and AFCs can be operated under ambient conditions, which allow their applications in our daily life, including electric vehicles and portable devices [10, 11, 12, 13]. Furthermore, the replacement of liquid electrolyte by solid polymer electrolyte (i.e., ion exchange membrane) can overcome the problems of electrolyte leakage and carbonate precipitation [14, 15, 16, 17, 18, 19]. The PEFCs can be divided into two types of fuel cell based on the employed membranes, i.e., anion exchange membrane fuel cells (AEMFCs) and proton exchange membrane fuel cells (PEMFCs) [20, 21]. Compared to PEMFCs, AAEMFCs have received ever-increasing attention recently, primarily due to the following advantages [22, 23, 24]: (1) faster electrochemical kinetics of the

ORR in alkaline media, (2) the absence of noble metal electrocatalysts leading to the lower cost, and (3) the alleviated fuel crossover from the anode to cathode by the directional electro-osmotic drag from the cathode to anode.

Typically, as hydrogen and oxygen have been employed as fuel and oxidant in an AAEMFC, respectively, the final products are electricity, heat, and water. This case is the most representative in electricity generation without pollution emission. However, the issues associated with hydrogen production, transportation and storage overshadow the commercialization of H₂/O₂ fuel cells [25]. Hence, liquid alcohols derived from biomass that are renewable, cheap, and abundant are expected to be employed as fuels fed into the anode chamber [26, 27]. To date, the complete electro-oxidation of alcohols including ethanol, ethylene glycol (EG), and glycerol to CO₂ has not been achieved under ambient conditions [28, 29, 30]. Although it remains a challenging task, the partial and selective electro-oxidation of polyalcohols provides a potential route to obtain valuable chemicals of industrial interest, such as tartrate, oxalate, and mesoxalate, etc. [31]. Particularly, mesoxalic acid that is 140 USD g⁻¹ is the precursor to synthesize an anti-human immunodeficiency (HIV) agent [32]. In addition, mesoxalate is applied in the treatment of diabetes [33]. Tartrate acid whose price is as high as 1536 USD g⁻¹ has been widely used in medicine industries [34], food industries [35, 36, 37], and anti-corrosive protective agents [38].

Hence, considerable researches have been conducted on simultaneous generation of electricity and valuable chemicals by using an AAEMFC and great progress has been made [39, 40, 41, 42, 43]. The objective of this review is to provide a general description of this type of device, summarize the various valuable chemicals and power output, introduce innovative system designs, as well as highlight the remaining challenges and future directions.

2. General description

In principle, the structure of AAEMFCs is just borrowed from PEMFCs, with the main difference that the solid membrane is an AAEM instead of a proton exchange membrane (PEM). In AAEMFCs, the charge carrier is OH^- transporting through the AAEM from the cathode to the anode, while H^+ works as charge carrier transporting through the PEM from the anode to the cathode in PEMFCs. Generally, the critical component of a single AAEMFC is membrane electrode assembly (MEA) sandwiched between anode and cathode bipolar plates, which consists of an anode, an AAEM, and a cathode, as shown in Fig. 1. Specifically, the integrated multi-layered structure is composed of an anode diffusion layer (DL), an anode catalyst layer (CL), an AAEM, a cathode CL, and a cathode DL sequentially. Particularly, the DLs of the anode and cathode show the identical construction, both of which consist of a backing layer (BL) based on carbon paper or carbon cloth and a micro-porous layer (MPL) comprised of

carbon powders mixed with hydrophobic polymer (typically PTFE). Additionally, the CLs are usually made of electrocatalysts mixed with ionomer, leading to the formation of triple-phase boundaries (TPBs) for electrochemical reactions. Typically, the functions of DL can be concluded as follows: (1) provide the support for the corresponding CL, (2) distribute the reactants uniformly, (3) realize the good water management, and (4) transport electrons to the current collector. The AAEM functions as a barrier to separate the anode and cathode, preventing the fuel crossover from the anode to cathode; meanwhile, it provides the pathway for conducting hydroxide ions. The released electrons by fuel electro-oxidation transport through the external circuit to complete the loop.

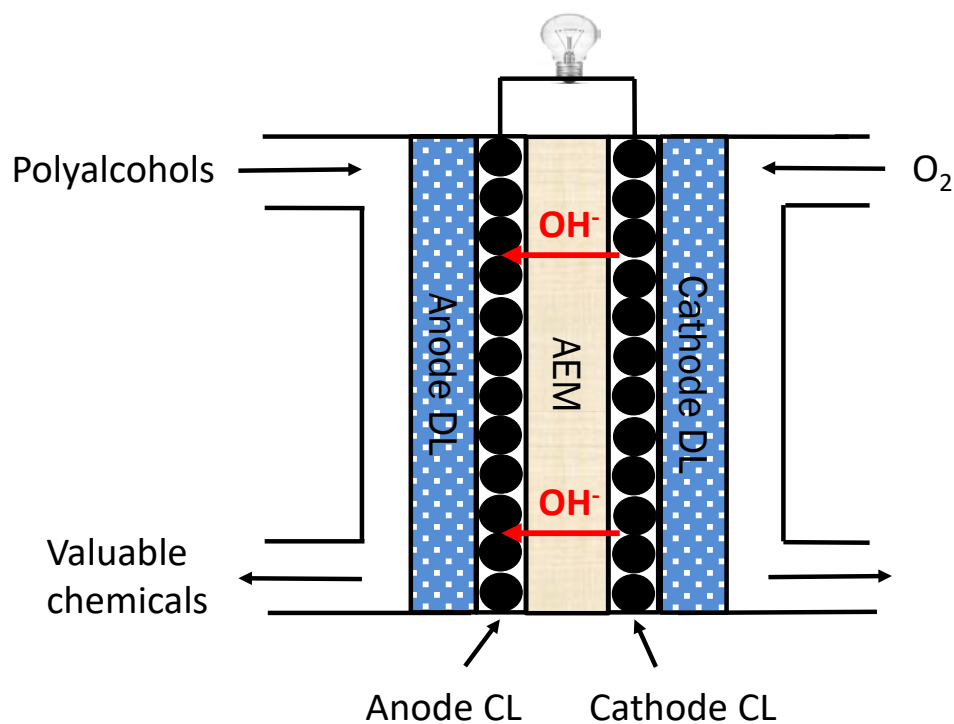


Figure 1 Schematic of a typical alkaline anion exchange membrane fuel cell (AAEMFC).

It is worth mentioning that the fuel supply method is quite different from the conventional AAEMFC for power generation. Since the selective conversion ratio is the most critical parameter that is associated with the yield of the target product and the amount of the initial provided fuel, the supplied solution containing fuel and alkali should be cycled between the solution vessel and the anode chamber via a closed loop, usually employing a peristaltic pump, for a certain time.

As EG and glycerol that are derived from biomass are the two simplest polyols, herein the discussion of the reaction mechanisms is limited to EG and glycerol electro-oxidation. The reaction pathways of EG and glycerol electro-oxidation are illustrated in Fig. 2 (a). It is indicated that electro-oxidation of EG can go through two reaction routes, either the poisoning paths or the non-poisoning paths [44]. The final products of non-poisoning route are oxalate, glycolate, and glycoxalate, and it ends at oxalate due to its slow electro-oxidation on the existing electrocatalysts. Although oxalate is not the main product, it can be obtained by further electro-oxidation of glycolate or glycoxalate depending on pH. The final product of poisoning route is formate derived from the cleavage of C-C bond of glycolate. It should be noted that the applied potential plays an important role in C-C bond scission. When the potential is lower than 400 mV, no C-C bond cleavage occurs on Pt electrocatalyst, and the C-C

bond of EG is cleaved at 500 mV, leading to CO poisoning [45]. It was reported by Demarconnay et al. [46] that the addition of Bi to Pt resulted in decreasing the onset potential of EG electrooxidation of about 70 mV and achieving higher current densities in the whole studied potential range. Furthermore, a ternary catalyst PtPdBi/C did not change the onset potential of EG oxidation, but increased the current densities compared to PtBi catalysts. It was shown from the results of fourier transform infrared spectroscopy (FTIR) that the addition of foreign atoms to Pt led to decreasing the ability of the catalyst to break the C-C bond. Nevertheless, catalysts containing Pd and Bi were more likely to activate the oxidation of EG in oxalate compared to pure Pt. It was proposed that Bi mainly favors the adsorption of OH species but also affected the product distribution by changing the composition of chemisorbed species, whereas Pd only limited the poisoning of Pt sites by changing the composition of chemisorbed species.

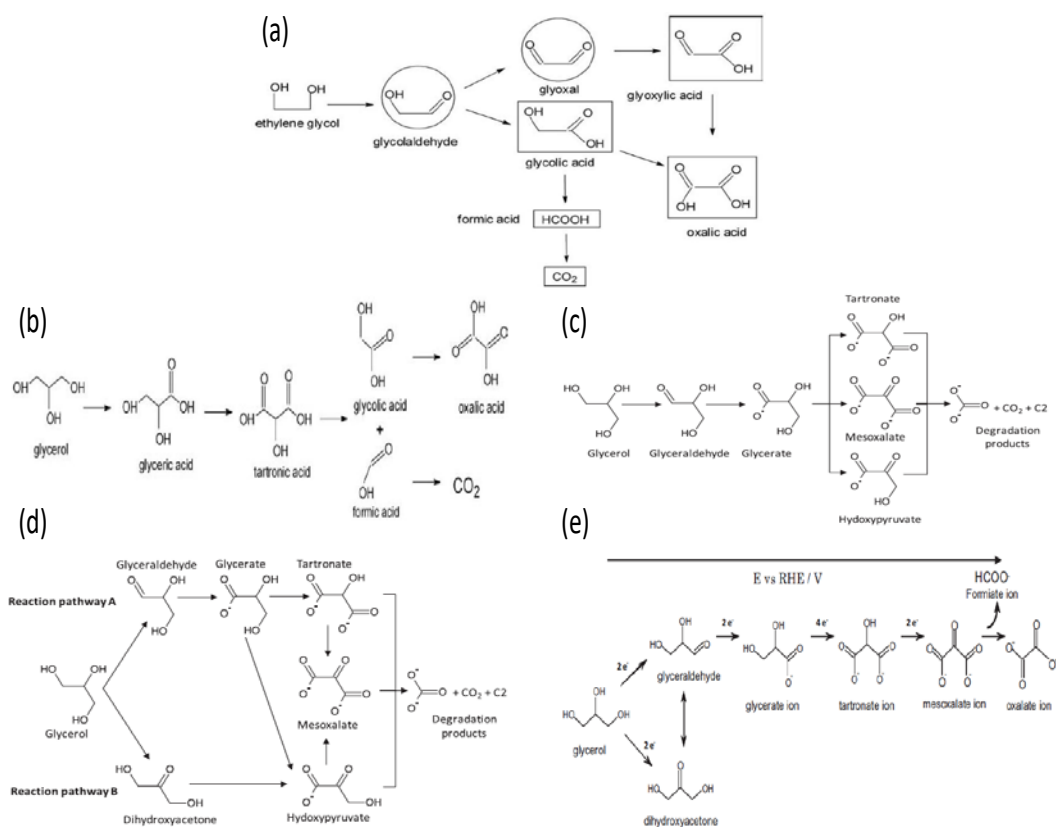


Figure 2 (a) Proposed mechanism for ethylene glycol electro-oxidation [44]. Reproduced with permission from American Chemical Society. (b) (c) (d) (e) Proposed mechanism for glycerol electro-oxidation [47] [48] [49]. Reproduced with permission from Elsevier.

Since glycerol possesses one more -OH group than EG, the electro-oxidation of glycerol is much complex, leading to tremendous efforts made in shedding light on the reaction mechanisms for electro-oxidation of glycerol. Bambagioni et al. [47] proposed that the first procedure is the electro-oxidation of the primary -OH group to yield glyceric acid. Then the second procedure is the electro-oxidation of the other end -OH group to form tartronic acid. Subsequently, the cleavage of C-C bond of tartronic acid occurs resulting in the formation of glycolic and formic acids. Finally, glycolic and formic acids will be further electro-oxidized to oxalic acid and CO_2 ,

respectively, as Figure 2 (b) illustrated. Zalineeva et al. [48] studied the glycerol electrooxidation on pure Pd nanoparticles (NPs) and Bi-modified Pd NPs via *in situ* FTIR. It was reported that glycerol was selectively electrooxidized to glyceraldehydes and glycerate at low potentials on pure Pd NPs, and at high potentials, tartronate, mesoxalate, hydroxypyruvate, and degradation products were formed as Figure 2 (c) showed. While the glycerol electrooxidation on Bi-Pd NPs was divided into two pathways as Figure 2 (d) expressed, reaction pathway A was similar to that of pure Pd NPs. The difference between pathway A and pathway B lied on the formation of dihydroxyacetone at low potentials, then the dihydroxyacetone was further electrooxidized to hydroxypyruvate, providing an alternative pathway for formation of hydroxypyruvate. For the reaction mechanism on ternary catalyst PdPtBi/C, Simoes et al. [49] proposed a possible route based on the *in situ* infrared spectroscopy measurements and high performance liquid chromatography (HPLC) combined with chronoamperometry as Figure 2 (e) depicted. At low overpotentials, the main products were glycerate, dihydroxyacetone, and tartronate. Further increasing the potentials, mesoxalate was detected, but no oxalate and formate were formed.

In summary, the above-mentioned reaction routes for EG and glycerol electro-oxidations are significantly affected by the employed electrocatalysts. Hence, it is critical to investigate the certain reaction mechanism on various electrocatalysts.

3. Various valuable chemicals

It is widely accepted that breaking the C-C bonds of polyols in an AAEMFC at low temperatures and low anode overpotentials is difficult to realize. Due to the incomplete electro-oxidation of polyols, several valuable chemicals can be obtained in the AAEM-DAFCs, which offer much greener process compared to current stoichiometric oxidation processes. Moreover, it is feasible to design electrocatalysts with high selectivity towards target product with high added-value, resulting in high conversion ratio. In addition, the production of bio-renewable polyols is more profitable due to the double income of electricity and valuable chemicals. Recently, considerable researches have been conducted on the strategy to simultaneously generate electricity and valuable chemicals [50, 51, 52, 53, 54]. The performances reported in recent literatures have been concluded in Table 1. The following subsections will discuss the various products through feeding different fuels into the AAEMFC.

3.1. Formate

Formate, one of basic organic raw materials, has been widely used in industry such as pesticide, leather, dye, medicine and rubber [55]. Hence, the selectivity of glycerol electro-oxidation towards formate has been studied [39, 50, 56]. Prasanna et al. [39] prepared a ternary polymer-carbon nanotube (CNT) composite that is composed of

amine terminated cyclophosphazene (ATCP), hexachlorocyclotri- phosphazene (CP) and 2,2'- benzidinedisulfonic acid (BZD), denoted as ATCP-CP-BZD-CNT. Then the composite was utilized as support for Pt and Pt-Sn NPs for electro-oxidation of glycerol. It was indicated that the NPs with size of ~2.0 nm were uniformly deposited on the base, resulting from three functional groups that were -NH, -HSO₃, and -O. The electrochemical test showed that the electro-oxidation current of Pt/ATCP-CP-BZD-CNT and Pt-Sn/ATCP-CP-BZD-CNT were 26.59 and 38.89 mA mg⁻¹, respectively, both of which were higher than those generated by using the Pt/C and Pt/CNT. In addition, the onset potentials of Pt/ATCP-CP-BZD-CNT and Pt-Sn/ATCP-CP-BZD-CNT were -0.64 V and -0.74 V, respectively, both of which were negative than those of the Pt/C and Pt/CNT, indicating the potential to be used as anode material due to its excellent electrocatalytic activity. It was demonstrated by Demarconnay et al. [46] that the electrooxidation of EG at Pt started at ca. 0.35 V and carbonate were formed from ca. 0.43 V vs reversible hydrogen electrode (RHE). On the other hand, the products of glycerol electro-oxidation on the two electrocatalysts were similar. The main product was formate with a conversion ratio of 70%, as well as 17% of glyceraldehyde and 13% glycolate. Oliveira et al. [50] synthesized Ni-based electrocatalysts via impregnation method for glycerol electro-oxidation in alkaline media. It was shown from the X-ray diffraction (XRD) patterns that the

crystallite sizes of the particles were ranged from 15 to 22 nm. It was indicated that the presence of Co and Fe in the binary and ternary Ni-based electrocatalysts was beneficial for glycerol electro-oxidation due to the formation of oxide and hydroxides and the shape change of the oxy-hydroxide region. The HPLC analysis demonstrated that the main product was formate, while glycerate, glycolate, tartronate, and oxalate were also observed. In addition, Ni/C and FeCoNi/C exhibited the best conversion ratio of glycerol to formate and glycolate, CoNi/C possessed the highest glycerol conversion ratio (17.9%) as well. Although the Ni-based electrocatalysts are not suitable to be used in power supply devices due to the extremely high anodic overpotential for glycerol electro-oxidation, it could be utilized as electrochemical reactor to produce valuable chemicals and electricity. Wang et al. [56] developed carbon nitride and graphene (CN_x/G) via annealing polypyrrole/GO at 800°C to support Pd NPs. The size of Pd loaded on CN_x/G was smaller than that on CN_x due to the larger surface area of CN_x/G . As a result of the smaller size and nitrogen interaction, the Pd- CN_x/G exhibited higher activity and better selectivity. Fig. 3 showed the results of product analysis and the mechanistic scheme of glycerol electro-oxidation. It could be seen that the main product was formate on the Pd/carbon black, whose concentration was ~15% higher than the total amount of glycolate and oxalate. It should be noted that the actual production of formate was higher than the

detected production due to the further conversion of formate to carbonate. However, the concentration of formate was decreased significantly on Pd-CN_x/G and the concentration of oxalate was increased, indicating that the path was suppressed and the conversion of glycolate to oxalate was encouraged. Meanwhile, it should be noted that the interaction between Pd and N atom played an important role in the selectivity towards C₃ products. It was demonstrated that the interaction weakened the adsorption ability of Pd towards C₃ products, leading to the less C₃ products being oxidized. In summary, a formate conversion ratio of 70% was achieved with 0.5 M glycerol fed as fuel as well as Pt-Sn/ATCP-CP-BZD-CNT employed as the anode electrocatalyst at a current of 38.89 mA, while the conversion ratio decreased to 34.1% with the utilization of non-precious metal electrocatalysts. Hence, we suggest that improving the selectivity of non-precious metal electrocatalysts be a critical future research direction.

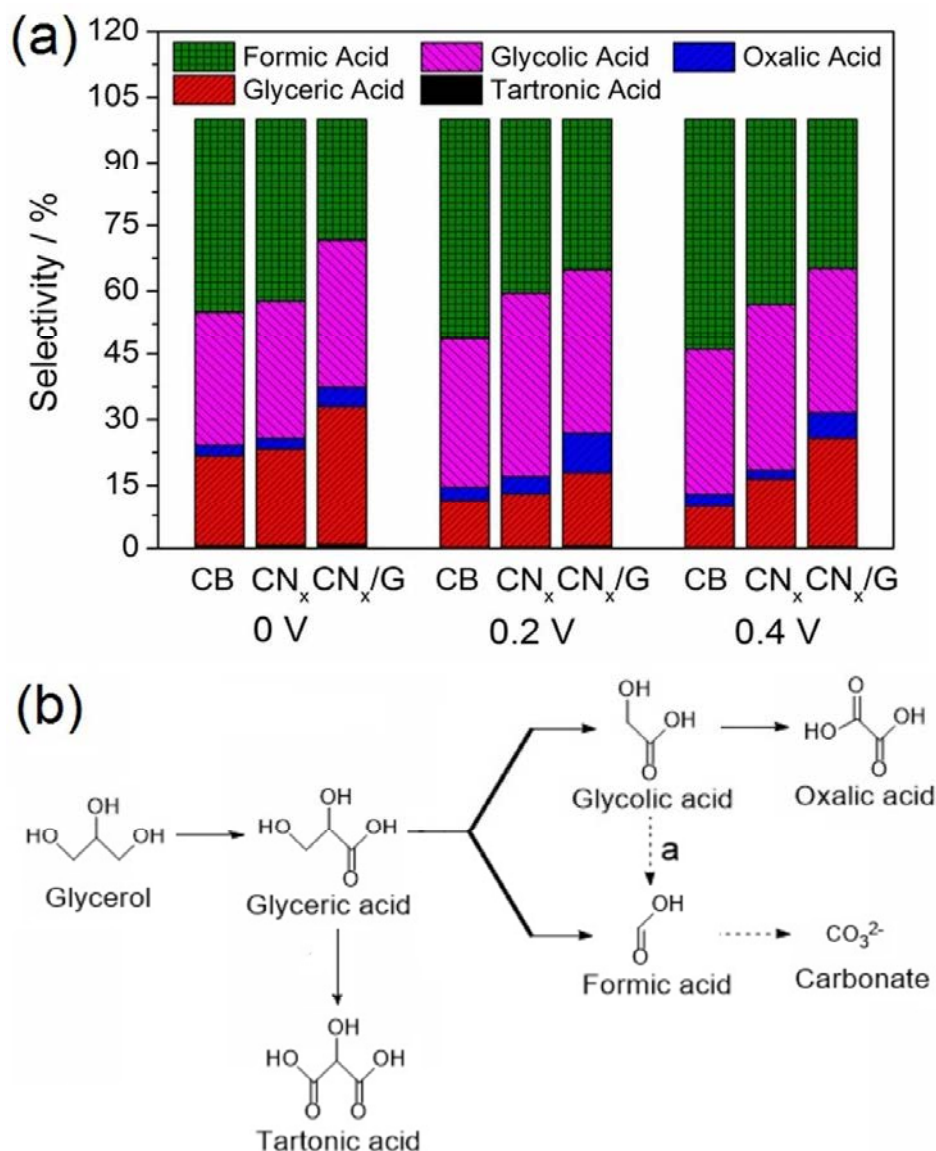


Figure 3 (a) The product selectivity of Pd NPs on different supports (CB, CN_x, CN_x/G) at various potentials. (b) The mechanistic of glycerol oxidation [56]. Reproduced with permission from American Chemical Society.

3.2. Oxalate

Oxalate, the conjugate base of oxalic acid, is an excellent ligand for metal ions. In addition, oxalate powder is used as a pesticide in beekeeping to combat the bee mite. Therefore, the selectivity of glycerol electro-oxidation to oxalate has been investigated [40, 51, 57]. Qi et al. [40] prepared PdAg/CNT electrocatalyst with an

average size of 2.7 nm via an aqueous phase reduction method, in which CNT acted as the support for PdAg. It was shown from the single fuel cell test that the peak power densities were 135.1 mW cm⁻², 202.3 mW cm⁻², 245.2 mW cm⁻², and 276.2 mW cm⁻² with methanol, ethanol, EG, and glycerol fed into anode, respectively, when PdAg/CNT were employed as the anode electrocatalyst. The half-cell system test implied that the peak mass activity of PdAg/CNT was higher than that of Pd/CNT under the same conditions, which could be attributed to the following reasons: (1) the inset of Ag could accelerate the reaction rate of alcohol direct oxidation reaction, (2) the particle size of alloyed electrocatalyst (2.7 nm) was much smaller than that of Ag/CNT (17.7 nm), resulting in a high electrochemically active surface area (ECSA), and (3) the CNT support not only provided 3D structure that enhances the mass transport of alcohol molecules and hydroxide ions, but also enhanced the electrical conductivity, as well as mechanical and thermal stabilities. Moreover, it was shown from the product analysis that the selective electro-oxidation of glycerol to oxalate was 8.6%, 22.8% and 46.6% on Pd/CNT, PdAg/CNT, and PdAg₃/CNT, respectively, indicating that Ag facilitated the C-C bond cleavage of glycerol to oxalate. Matsumoto et al. [51] synthesized a FeCoNi ternary nanoalloy (NA) electrocatalyst via a two-step reduction method as shown in Fig. 4. It was indicated that the electrocatalyst exhibited highly selective EG oxidation to C₂ products with a conversion ratio of 99%, in which

oxalate occupied 60% at 0.4 V vs. RHE. Subsequently, the FeCoNi electrocatalyst was used in an AAEMFC in the absence of any precious metal, showing a peak power density of 34 mW cm^{-2} , which was three times higher than that using the bare Fe (10 mW cm^{-2}) at 70°C . Nevertheless, it was essential to avoid the self-oxidation of Fe, thereby enhancing the stability and lifetime of electrocatalysts. Benipal et al. [57] developed Pd and Ag bimetallic nanoparticles loaded on CNT electrocatalysts (PdAg/CNT, and Pd₁Ag₃/CNT) for selective electro-oxidation of glycerol in an AAEMFC via an aqueous-phase reduction method. The TEM patterns showed that the particle sizes of Pd/CNT, Ag/CNT, PdAg/CNT, and Pd₁Ag₃/CNT were 2.0 nm, 13.9 nm, 2.3 nm, and 2.4 nm, respectively. It was indicated from the single fuel cell test results that the bimetallic electrocatalyst facilitated the glycerol oxidation leading to a higher power output. The product analysis conducted in an AAEMFC at a constant voltage of 0.1 V at 60°C showed that the selectivity towards oxalate was increased with increasing the Ag content, indicating that Ag contributed to the cleavage of C-C bond.

In summary, an oxalate conversion ratio of 40% was obtained when 1 M glycerol was fed into anode and PdAg/CNT was used as the anode electrocatalyst at 0.2 V vs. RHE for 4 h at 80°C . Although the conversion ratio was promising, the high cost derived from the employment of precious metal electrocatalysts impeded the

commercialization. We recommend that future research focus should be paid on reducing the cost of the electrocatalysts.

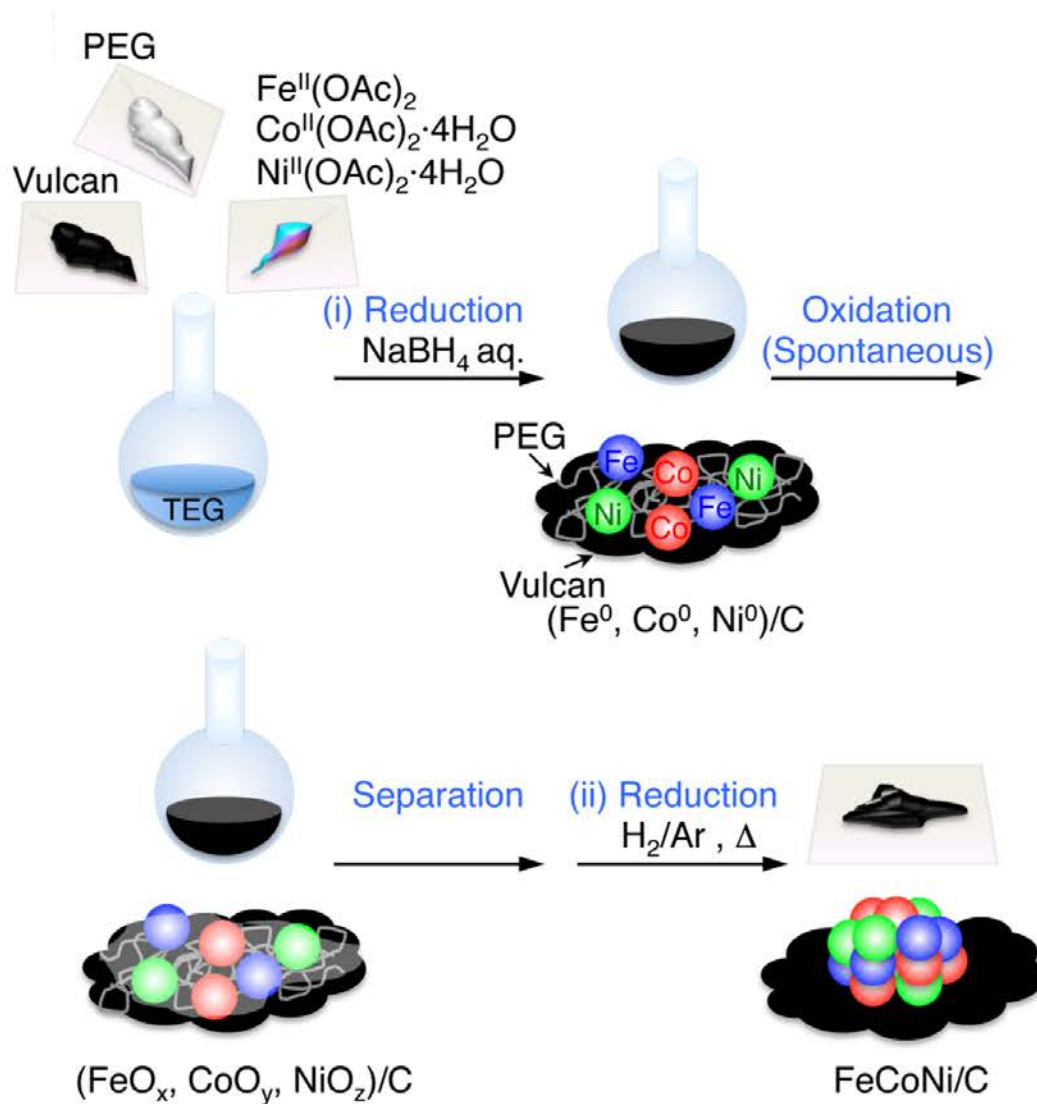


Figure 4 Scheme of the preparation of a FeCoNi nanoalloy catalyst loaded on carbon [51]. Reproduced with permission from Nature Publishing.

3.3. Glycolate

Glycolate has been widely used in synthesizing other organic compounds. Hence, the selectivity towards electro-oxidation of EG and glycerol to glycolate has been studied [41, 52, 58]. Marchionni et al. [41] synthesized Pd NPs loaded on a Ni-Zn phase with

an average diameter of 2.3 nm for electro-oxidation of EG. It was indicated that Pd-(Ni-Zn)/C was more active and less selective than Pd/C towards EG electro-oxidation. The total EG conversion ratio on Pd-(Ni-Zn)/C was 77.1%, which was higher than that on Pd/C (55.5%). The selective glycolate conversion ratio on Pd-(Ni-Zn)/C was 55.4%, which was lower than that on Pd/C (89.5%). The excellent electrocatalytic activity was ascribed to the well dispersed metal particles and intrinsic properties of the Ni-Zn phase. Zhang et al. [52] synthesized Au/CNT for highly selective electro-oxidation of glycerol to glycolate at 1.6 V vs. standard hydrogen electrode (SHE) under ambient conditions with water as solvent. It was demonstrated that the selectivity was affected by the applied potentials and higher applied potentials resulted in higher selectivity to glycolate as shown in Fig. 5 (a). At an applied potential of 1.0 V, glycolate selectivity was only 14%, while the applied potential was 1.6 V, the selectivity could reach up to 85%. They claimed that at low potentials, glycerol was preferred to be oxidized to tartronate, further to mesoxalate. However, at high potentials, the cleavage of C-C bond was dominated, leading to the high selectivity of glycolate. In addition, the effect of reaction time on the final products was finite. Fashedemi et al. [58] prepared ternary core-shell nanoparticles (FeCo@Fe@Pd) loaded on MWCNT-COOH and MWCNT-SO₃H for electro-oxidation of EG and glycerol. It was determined that the

FeCo@Fe@Pd/MWCNT-COOH possessed smaller nanoparticles, which were more evenly loading on the support, large active surface area, and enhanced electrocatalytic activity. For the EG electro-oxidation, FeCo@Fe@Pd/MWCNT-COOH exhibited remarkable selective electro-oxidation to carbonate (67%) and glycolate (28%), while the total conversion reached 65% and the released energy was 551 J for 8.7 h, which was kind of inferior compared to the work that Qi et al. [42] selectively oxidized glycerol to tartronate using Au/C (1527 J). Pd/MWCNT-COOH showed higher EG electro-oxidation selectivity to glycolate (65 %), but both the total conversion ratio (29%) and released energy (67 J) were lowered. For the glycerol electro-oxidation, both FeCo@Fe@Pd/MWCNT-COOH and Pd/MWCNT-COOH showed significant selectivity to oxidize glycerol to carbonate, reaching 73% and 47%, respectively. Moreover, the oxidation products were diverse compared to EG, including formate, oxalate, glycolate, tartronate, and glycerate.

In summary, an extremely high conversion ratio of EG to glycolate (89.5%) was achieved with 5 wt. % EG as fuel and Pd/C as the anode electrocatalyst at 20 mA cm^{-2} for 10.2 h. It should be noted that it took a very long time (10.2 h) to realize the excellent conversion ratio, indicating that the reaction rate was quiet low. Hence, future attention can be paid on reducing the reaction time to make the progress more efficient.

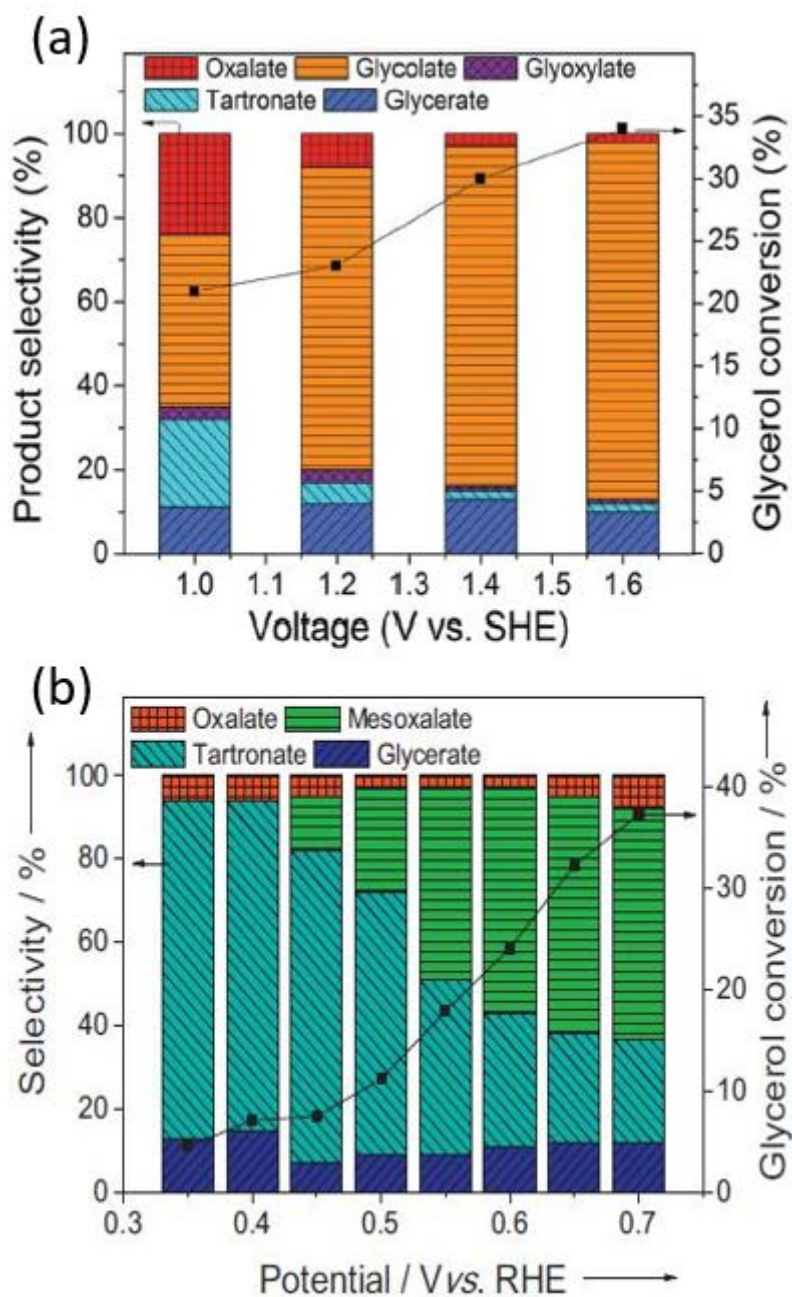


Figure 5 (a) The product selectivity of glycerol electro-oxidation on Au/CNT at various potentials [52]. Reproduced with permission from The Royal Society of Chemistry. (b) The product selectivity of glycerol electro-oxidation on Au/C at various potentials [59]. Reproduced with permission from Elsevier.

3.4. Tartronate

Tartronate has been widely used in medicine industries [34], thus efforts have been paid to improve the selectivity of glycerol electro-oxidation to tartronate [42, 53, 59].

Qi et al. [42] prepared Au/C for selectively oxidizing glycerol to tartronate. A high tartronate yield of 61.8% and released energy of 1527 J were achieved in an AAEMFC. It was revealed that the anode potential should be tuned to < 0.45 V that was preferable to oxidize two primary -OH groups, avoiding over-oxidation of the secondary -OH and cleavage of C-C bond, thereby promoting the tartronate selectivity. Furthermore, optimal MEA structure, flow rate, operating temperature, and pH could improve the mass transport to enhance the reaction kinetics and accelerate the desorption rate of produced tartronate from active sites. Meanwhile, they synthesized two Au/C electrocatalysts via nanocapsule method (Au/C-NC) and aqueous-phase reduction method (Au/C-AQ). It was claimed that the glycerol conversion ratio of Au/C-AQ (95.6%) was slightly higher than Au/C-NC (89.2%), but the tartronate yields were close (61.2% of Au/C-AQ and 61.8% Au/C-NC). Zhang et al. [53] synthesized Pt/C catalysts with a size distribution of 1-4 nm via a solution phase-based nanocapsule method. It was indicated that this electrocatalyst exhibited excellent selectivity (91%) of C_3 products at 0.7 V with 2 M KOH and 0.1 M glycerol, in which tartronate and glycerate occupied 50% and 41%, respectively. In addition, increasing the pH resulted in the enhancement of power density and conversion ratio to C_3 products. Decreasing the glycerol concentration could lead to higher selectivity of deeper-oxidized products (oxalate and mesoxalate). They also found that high

anode overpotentials facilitated the cleavage of C-C bond. Therefore, the selectivity of C₃ products was lower. Similarly, Zhang et al. [59] demonstrated that the selectivity of glycerol electro-oxidation could be controlled by tuning the anode potentials, as shown in Fig. 5 (b). When the anode potential was increased from 0.35 V to 0.65 V, the tartronate yield was decreased from 79% to 26%, while the mesocalate yield increased from 0% to 57%. It was claimed that the process of oxidizing two primary -OH groups was dominant in the range of 0.35 V to 0.45 V, resulting in the selective production of tartronate. From 0.45 V to 0.9 V, three -OH groups were oxidized to form mesoxalate, and above 0.9 V, the cleavage of C-C bond was preferred, thus the glycolate was selectively produced.

In summary, the conversion ratio of glycerol to tartronate reaching 80% was realized with 1 M glycerol as fuel and Au/C as the electrocatalyst at 0.35 V vs. RHE for 1 h at 50°C. In the future, the research focus should be paid on reducing the cost of the electrocatalysts.

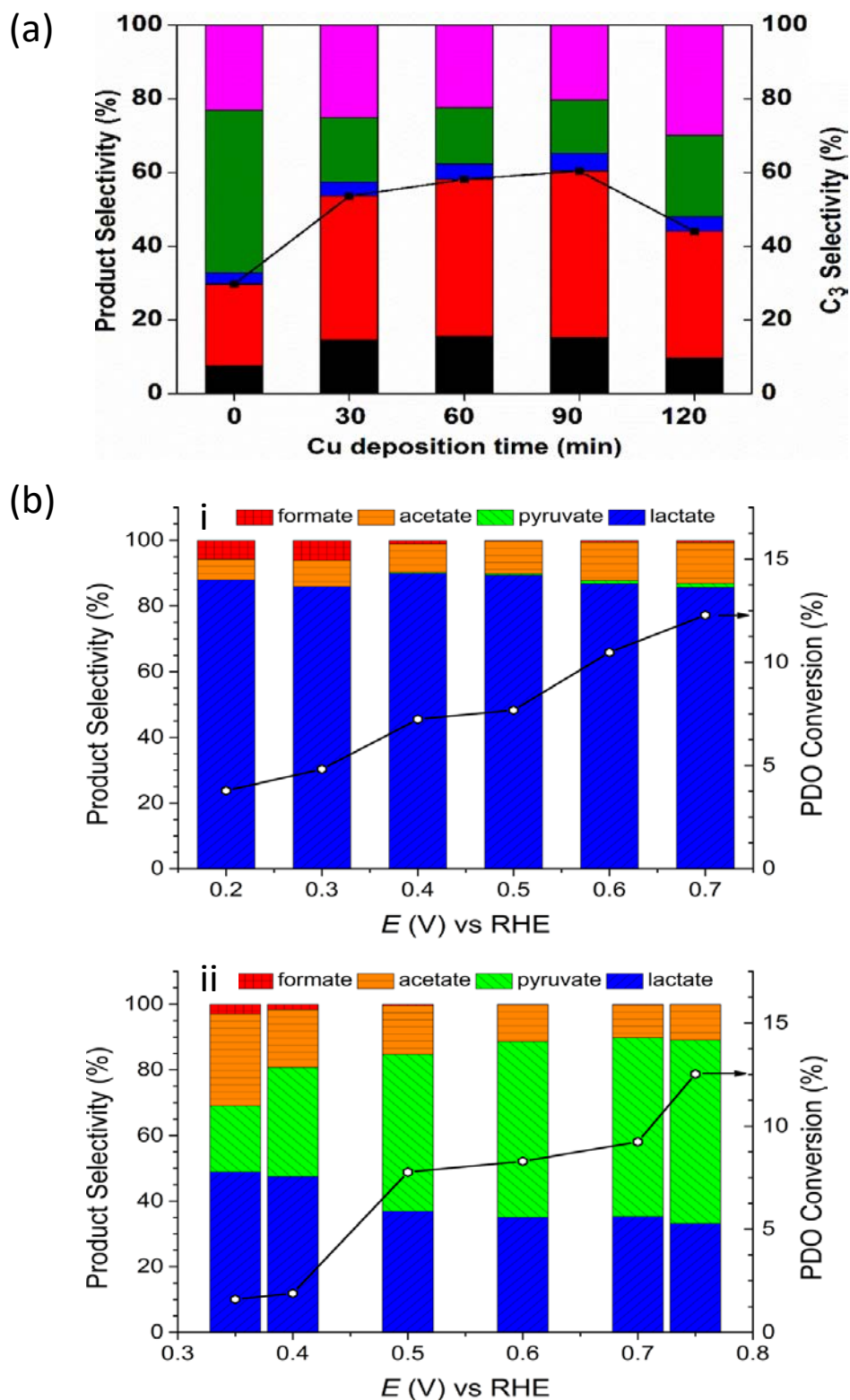


Figure 6 (a) Product selectivity during glycerol electro-oxidation over catalysts prepared at +0.015 V for different durations. Formate=■, glycolate=■, oxalate=■, glycerate=■, tartronate=■ [43]. Reproduced with permission from Wiley. (b) The product selectivity of PDO electrooxidation on (i) Pt/C and (ii) Au/C at various potentials [62]. Reproduced with permission from American Chemical Society.

3.5. Glycerate

Glycerate is an important molecule for the biosynthesis of serine, which can be used for the synthesis of cysteine and glycine. It has been investigated to promote the selectivity of glycerol towards glycerate [43,54]. Thia et al. [43] promoted the C₃ selectivity of Au/C for glycerol electro-oxidation by electro-deposited Cu species. Fig. 6a showed the effects of deposition time on the product selectivity at +0.015 V. It could be seen that the C₃ selectivity was increased with increasing the deposition time from 0 min to 90 min, and after 90-min electro-deposition of Cu at +0.015 V, the C₃ selectivity increased to 60%, which was twice as that without deposition, indicating that the cleavage of C₃ products to form C₂ products was suppressed. In addition, the production of glycerate that was one of the C₃ products occupied 45%. However, further increasing deposition time to 120 min, the selectivity was significantly decreased due to the formation of thick Cu layer over the Au/C hindering the adsorption of C₃ products from the electrocatalyst surface. Hence, the C-C bond of the trapped C₃ products would be broken to form C₂ products for a long time. Wang et al. [54] synthesized Au NPs loaded on four materials that were carbon black (Au-CB), poly(4-vinylpyridine) functionalized graphene (Au-P4P/G), P4P functionalized reduced graphene oxide (Au-P4P/rGO), and poly(m-aminophenol) (PmAP) wrapped graphene (Au-PmAP/G) for the selective electro-oxidation of

glycerol. It was shown from the off-line HPLC analysis that the Au-P4P/G possessed better selectivity for the C₃ products than other three electrocatalysts. A high conversion ratio of glycerol to glycerate (68.6%) was achieved at 0.2 V vs. HgO/Hg, and the ratio between C₃ products and other products on Au-P4P/G (4.92) was as almost five times as that of Au-CB. The superior selectivity for C₃ products was attributed to the lowest d-band center in Au-P4P/G derived from the extended P4P chain on graphene surface, which made the desorption of glycerate from Au surface much easier, preventing the glycerate being further decomposed to C₂ products.

In summary, a conversion ratio of 68.6% for electro-oxidizing glycerol to glycerate was obtained at 0.2 V vs. HgO/Hg for 2 h when 0.5 M glycerol and Au-P4P/G were used as fuel and electrocatalyst, respectively. As the electrocatalyst is composed of Au (1 mg cm⁻²), to further reduce the amount of Au used can be the future research focus.

3.6. Others

In addition to the above-mentioned products, other final products with high added-value have been extensively reported, including hydroxypyruvate [60], mesoxalate [61], pyruvate or lactate [62], dihydroxyacetone (DHA) [63], and alkali [64]. Simoes et al. [60] prepared Pd_{0.3}Au_{0.7}/C, Pd_{0.5}Au_{0.5}/C, and Pd_{0.5}Ni_{0.5}/C for electro-oxidation of glycerol. It was shown from the TEM patterns that the average size of bimetallic electrocatalysts was 5 nm, which was larger than that of

monometallic Pd (4 nm). It was indicated that the order of activity for bimetallic electrocatalysts was $\text{Pd}_{0.3}\text{Au}_{0.7}/\text{C} > \text{Pd}_{0.5}\text{Au}_{0.5}/\text{C} > \text{Pd}_{0.5}\text{Ni}_{0.5}/\text{C}$. They demonstrated that the electrocatalysts had remarkable effects on the glycerol electro-oxidation mechanism so that different final products could be obtained. It was determined by the *in-situ* infrared spectroscopy measurements that no adsorbed CO species was observed on the Au and $\text{Pd}_{0.3}\text{Au}_{0.7}$ surface, indicating that the cleavage of C-C bond was not occurred. Particularly, hydroxypyruvate, which was a valuable chemical, was detected on pure Au electrocatalyst. Xin et al. [61] prepared Au/C electrocatalyst with an average size of 3.5 nm via a solution phase reduction method. Then an AAEMFC fabricated with Au/C anode and Fe-Cu-N₄/C cathode exhibited a peak power density of 57.9 mW cm⁻² at 80°C. Meanwhile, high value-added mesoxalate was obtained by electro-oxidation of glycerol with high selectivity of 46% at the anode potential of 0.53 V vs. SHE. In contrast, the production of mesoxalate was negligible (< 3%) when Pt/C was employed as the anode electrocatalyst. It was demonstrated that the selectivity of mesoxalate was highly dependent on the anode overpotential, which means the selectivity decreased with increasing the anode potential. In addition, it was confirmed from the comparison between fuel cells and electrolysis that Au was beneficial for the complete electro-oxidation of glycerol to mesoxalate under mild potential range that was 0.4-0.7 V vs. SHE. Chadderdon et al. [62] proposed that 1,

2-propanediol (PDO) could be selectively electro-oxidized to pyruvate and lactate with Au/C and Pt/C as anode electrocatalysts in an AAEMFC, respectively. It was indicated that the conversion ratio of PDO to lactate in an AAEMFC fabricated with Pt/C as the anode electrocatalyst was as high as 86.8% accompanied with a peak power density of 46.3 mW cm⁻². Moreover, the further electro-oxidation of lactate to pyruvate occurred slowly on Pt/C. In addition, they found that the effects of anode potentials on the selectivity of pyruvate were significant. The selectivity towards lactate was 20.1% at 0.35 V, while increasing the potential to 0.75 V, the selectivity was improved to 55.9% as shown in Fig. 6b. It was explained that as long as the intermediates hydroxyacetone and pyruvaldehyde were trapped within the catalyst layer, they could be deeply electro-oxidized to pyruvate on Au due to their inferior stability under high pH condition. Palma et al. [63] developed Ru based Pd and Pt NPs for electro-oxidation of glycerol via a microwave assisted-heating technique. It was shown from the results of XRD and TEM that the Ru addition reduced the particles size and the average size of NPs that were in the range of 2 nm to 5 nm. It was confirmed by the chronopotentiometric and chronoamperometric measurements that both the electrocatalysts were stable at low potentials and effective for glycerol electro-oxidation due to the sufficient active sites. They demonstrated that one of the primary -OH groups of glycerol adsorbed on Pd-Ru/C encouraged the conversion of

glycerol to glyceraldehyde and then to glycerate via a four-electron transfer process, while adsorption by the secondary -OH on Pt-Ru/C promoted the selective conversion of glycerol to DHA, which was a high added-value chemical via a two-electron transfer process. Recently, Li et al. [64] proposed a direct formate fuel cell (DFFC) that not only generated electricity, but also produced NaOH. Hence, this type of fuel cell did not rely on the added base in the operation. The DFFC exhibited excellent stability operating for 13 h at a constant current of 10 mA, and yielded a peak power density of 33 mW cm⁻² at 60°C accompanied with the production of 195 mg NaOH. It was indicated that the hydrolysis of formate was attributed to the feasibility of this DFFC. González-Cobos et al. synthesized Bi-modified Pt catalysts for C3 alcohols electrooxidation [65] and electrochemical reforming of polyols into hydrogen and valuable chemicals [66], respectively. In both of the cases, the Pt NPs modified with 10 at. % Bi exhibited the best activity. It was indicated that the onset potentials of C3 electrooxidation decreased to ca. 0.2 V vs RHE, which was attributed to the Pt₉Bi₁/C catalyst possessing much higher electrocatalytic activity at low potentials. Moreover, the addition of Bi contributed to avoiding the C-C bond cleavage. Hence, the formation of valuable C3 products were favored. As for reforming of polyols, Pt₉Bi₁/C was also the most most active catalyst, resulting in the onset potential as low as 0.3 V vs RHE. Despite the formation of similar C3 products, a hydrogen

production of 0.11 and 0.23 Nm³H₂ h⁻¹ m⁻² was obtained with an energy consumption of 1.3 and 1.65 kWh (Nm³H₂)⁻¹ at 0.55 V and 0.7 V, respectively.

In summary, tremendous effects have been made in developing electrocatalysts for high selectivity towards valuable chemicals, such as formate, oxalate, glycolate, tartronate, and glycerate, all of which are derived from EG and glycerol. In addition to the effect of the electrocatalysts, the anode potential plays an important role in the selectivity. It should be noted that although the existing electrocatalysts possess reliable performance, the cost is still one of the obstacles for widespread applications because they are almost precious metal based electrocatalysts. Hence, it is critical to develop non-precious metal electrocatalysts with promising selectivity towards valuable chemicals.

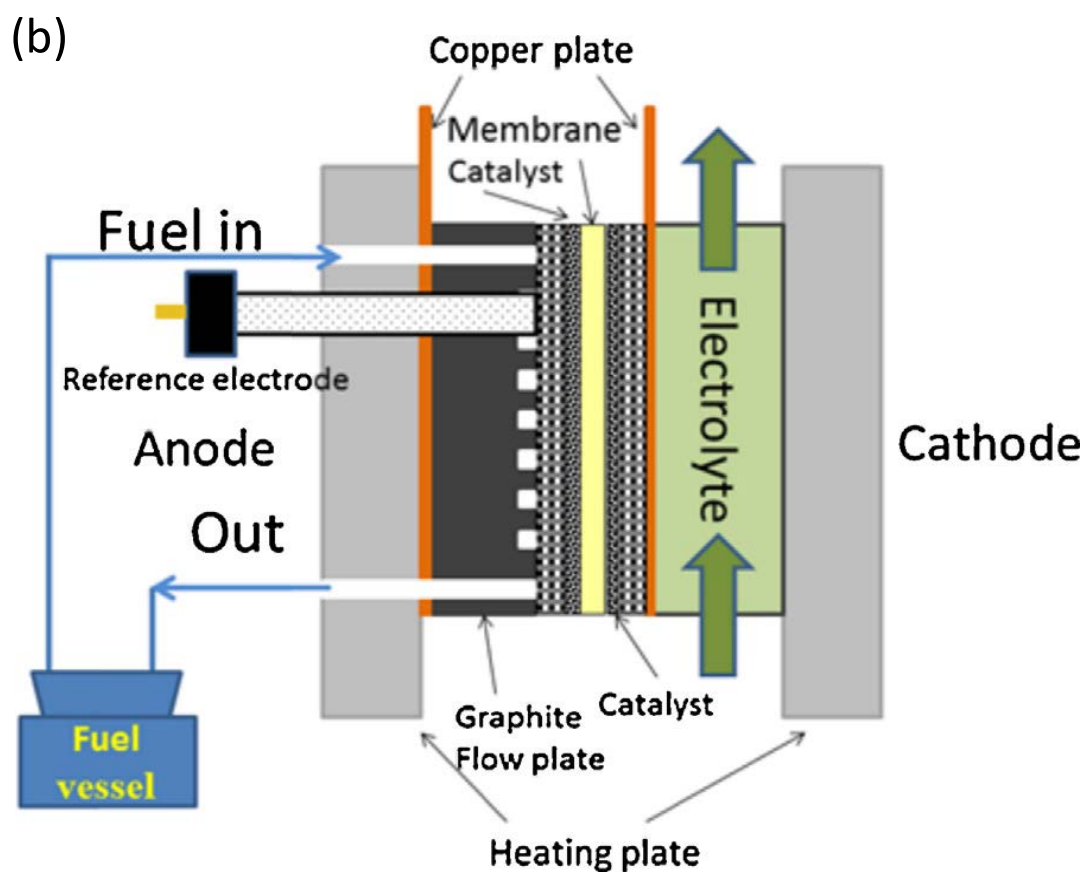
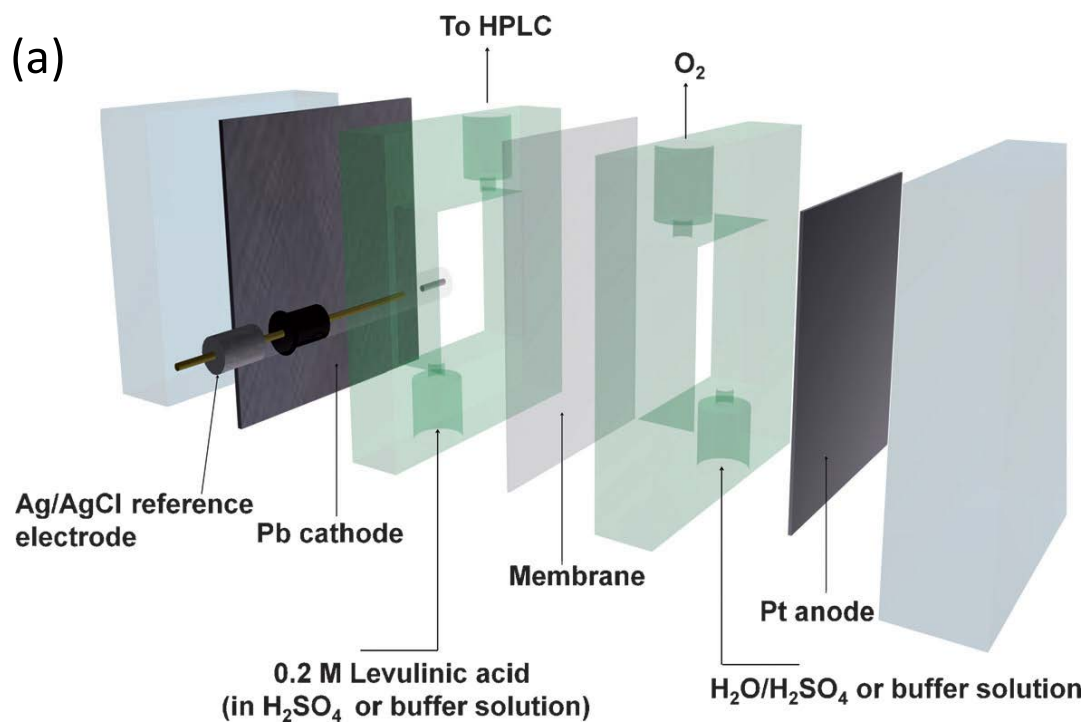


Figure 7 (a) Schematic of a single electrocatalytic (flow) cell reactor [67]. Reproduced with permission from Wiley. (b) Schematic of the anion exchange membrane-based electrocatalytic flow reactors [59]. Reproduced with permission from Elsevier.

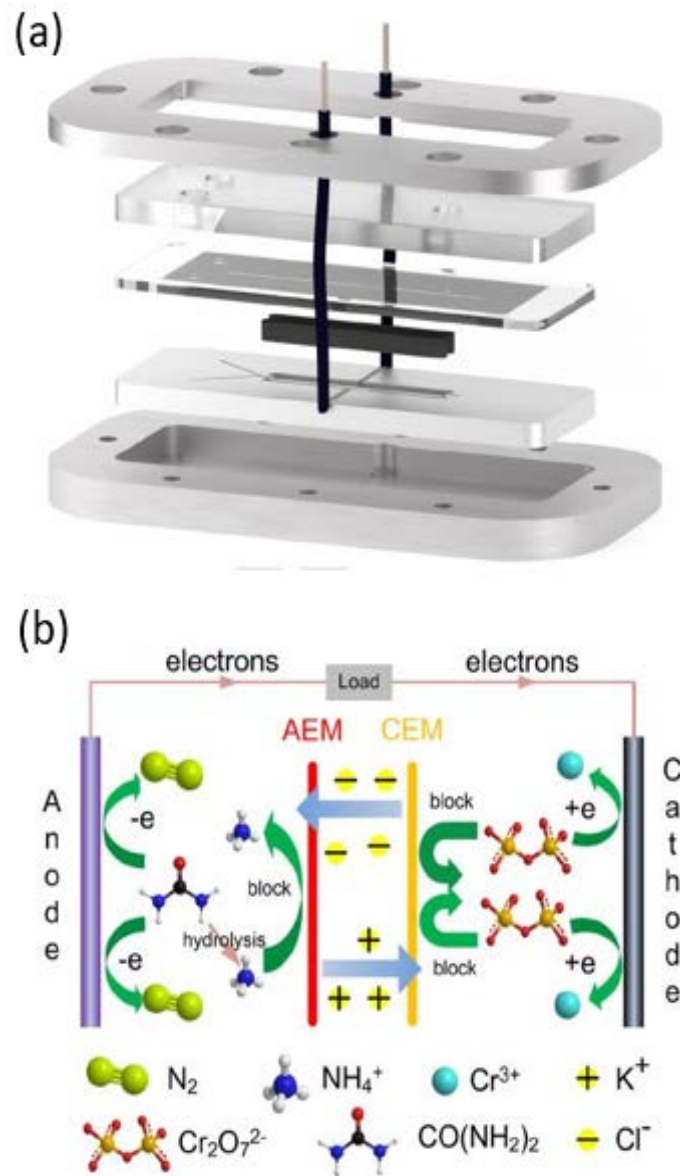


Figure 8 (a) Schematic of a typical laminar flow fuel cell [68]. (b) Schematic of a typical urine/Cr(VI) fuel cell [76]. Reproduced with permission from Elsevier.

4. Innovative system designs

In addition to the general construction of AAEMFC that has been introduced in Section 2, several innovative system designs have been proposed [58, 67, 68]. Xin et al. [67] reported a single-polymer electrolyte membrane electrocatalytic cell reactor that is composed of non-precious Pb electrode for efficient conversion levulinic acid

(LA) to valeric acid (VA) or γ -valerolactone (gVL). Fig. 7a depicts the structure of the reactor. The electrocatalytic hydrogenation (ECH) in this reactor did not require an external supply for hydrogen, but use the hydrogen generated *in-situ* on the surface of metal electrodes. Hence, the demand for high temperatures (370-420 K) and pressures (10-30 bar) to enhance the mass transport could be eliminated. It was indicated that a promising production of VA (> 90%), a high Faradaic efficiency of > 86%, and a remarkable electricity storage efficiency (70.8%) were achieved employing this reactor. The selectivity for VA and gVL was highly dependent on the applied potential and electrolyte pH. The formation of gVL was favorable under low overpotentials, while the production of VA was facilitated at high overpotentials. In addition, the selectivity for VA was 95% at pH=0, whereas the selectivity for gVL was 100% at pH=7.5. Similarly, Zhang et al. [58] developed an AEM electrocatalytic flow reactor, as shown in Fig. 7b. A porous liquid diffusion electrode (thickness > 700 μm , consisting of carbon cloth substrate: 381 μm and catalyst layer: 324 μm) was employed as conductive substrate. A confined electrolyte volume of 8 mL 2.0 M KOH + 1.0 M glycerol solution was continuously looped from the fuel vessel into the anode, and was allowed to react at 50°C at a certain applied potential. Wouters et al. [68] proposed a microfluidic fuel cell based on the laminar flow fuel cell design for cogeneration of electricity and aniline, as illustrated as Fig. 8a. Due to the

microfluidic structure, the membrane could be eliminated leading to the reduced cost. Despite the advantage of lower cost, the membraneless construction possessed other superiorities including flexible assembly [69], easy water management [70], and electrolyte pH flexibility [71]. It was reported that this reactor could serve for the hydrogenation of nitrobenzene with a small amount of electricity generation. A peak power density of 0.542 mW cm^{-2} was obtained when 0.0375 M nitrobenzene was fed at a flow rate of $55 \text{ }\mu\text{L min}^{-1}$. The highest conversion ratio of 74.0% could be achieved with the 0.0125 M nitrobenzene fed at a flow rate of $5 \text{ }\mu\text{L min}^{-1}$. It was demonstrated that the nitrobenzene concentration, the flow rate and the measurements themselves could affect the performance. A high nitrobenzene concentration enhanced the crossover that referred to the nitrobenzene diffusion from the cathode to anode, resulting in the nitrobenzene loss. Although the nitrobenzene loss increased with higher nitrobenzene concentration, the negative effects caused by the loss of nitrobenzene could be decreased due to the presence of much higher nitrobenzene concentration in the cathode. As the nitrobenzene concentration was a low flow rate slowed down the cathodic kinetics, which was ascribed to the combined effect of nitrobenzene deficiency and fuel crossover. The measurements could lead to the adsorption of CO on the surface of anode, poisoning the electrocatalysts.

In summary, a majority of the systems for cogeneration of electricity and valuable

chemicals are as the same as AAEMFCs. Although several novel system designs including flow reactors and microfluidic reactors have been proposed, the researches on this field are still limited. Hence, we suggest that more attention should be focused on developing innovative system designs with the high efficiency and low cost.

5. Removal of heavy-metal ions

Apart from cogeneration of electricity and valuable chemicals, AAEMFC can be used to remove toxic heavy-metal ions with electricity generation simultaneously. Herein, we take hexavalent chromium as a representative example to discuss. As Cr(VI) has been widely utilized in industries including metal finishing, chrome tanning, and petroleum refining [72], the industrial wastewater may contain abundant Cr(VI). Since the Cr(VI) possesses mutagenicity and carcinogenicity, the wastewater must be treated before being emitted to natural environment [73]. It is believed that the Cr(III) did not exhibit the toxicity. Hence, reducing Cr(VI) to Cr(III) is a promising way to alleviate the harmful effects on environment caused by Cr(VI) [74]. Virtually, converting Cr(VI) to Cr(III) is a redox reaction, which also exists in a fuel cell. Therefore, the strategy using fuel cell to deal with the Cr(VI)-containing wastewater accompanied with electricity generation has been proposed [75, 76, 77]. Zhang et al. [75] developed an alkaline fuel cell with ethanol fed into the anode as fuel and Cr(VI) containing solution fed into the cathode as oxidant to handle the Cr(VI) reduction. It

was indicated that increasing the initial Cr(VI) concentration could increase the removal efficiency and cathodic efficiency. Removal efficiency refers to the ratio of the removed Cr(VI) concentration and the initial Cr(VI) concentration, and cathodic efficiency refers the ratio of the theoretical generation electricity of Cr(VI) reduction and the total generation electricity. When the Cr(VI) concentration increased from 0.55 mM to 3.94 mM, the removal efficiency increased from 89.1% to 96.0%. In addition, the removal efficiency was improved from 64.6% to 83.3% with the H⁺ concentration increasing from 0.1 M to 1.0 M. The cathodic efficiency was promoted from 24.86% to 63.15% as the Cr(VI) concentration increased from 0.5 mM to 3.94 mM. Due to the presence of oxygen in the system that occupied the electrons for Cr(VI) reduction, the cathodic efficiency could not reach 100%. The peak power density was improved from 0.057 mW cm⁻² to 0.19 mW cm⁻² when the Cr(VI) concentration increased from 0.96 mM to 8.65 mM. When the H⁺ concentration increased from 0.1 M to 1.0 M, the peak power density was promoted from 0.026 mW cm⁻² to 0.071 mW cm⁻². Xu et al. [76] developed a urine/Cr(VI) fuel cell (UCrFC) for achieving reducing Cr(VI) and generating electricity simultaneously. Fig. 8b illustrated the configuration of the UCrFC, which was composed of a Ni based anode, an AAEM, a cation exchange membrane (CEM), and a cathode made of carbon cloth. The hybrid membrane functioned as a barrier preventing Cr(VI) and NH₄⁺ crossover.

A peak power density of 3400 mW m^{-2} was achieved with neat urine fed into the anode and 50 mg L^{-1} Cr(VI) and $0.25 \text{ M H}_2\text{SO}_4$ fed into the cathode. Additionally, the performance could be further improved by increasing the concentration of Cr(VI) and acids. It was indicated that after operating for 71 h, the removal efficiency of total organic carbon (TOC), total nitrogen (TN), and Cr(VI) was 79.2%, 78.4%, and 93%, respectively. Zhang et al. [77] proposed that a phenol-Cr(VI) coupled redox fuel cell could remove the phenol and Cr(VI) efficiently without energy input. Phenol was oxidized on Ni/C anode to release electrons, and Cr(VI) was reduced to Cr(III) by receiving the electrons transported through the external circuit. A peak power density was obtained with 0.94 g L^{-1} phenol in 0.2 M phosphate buffer solution (PBS) fed into the anode chamber and 0.15 g L^{-1} Cr(VI) in $0.5 \text{ M H}_2\text{SO}_4$ fed into cathode chamber. It was indicated that the removal efficiency of phenol was 98.6% within 132 h, and removal efficiency of Cr(VI) was 99.8% within 60 h.

In summary, employing an AAEMFC to reduce Cr(VI) to Cr(III) is a novel strategy in dealing with industrial wastewater containing toxic Cr(VI) ions. Though the removal efficiency is relatively high, as an emerging technology that simultaneously generates electricity and reduces Cr(VI), the power output is negligible. Hence, future research direction should be focused on improving the peak power density of this type of reactor.

6. Concluding remarks

The concept that cogenerates electricity and valuable chemicals in alkaline anion exchange membrane fuel cells has attracted worldwide attention recently, because it kills two birds with one stone. Consequently, great progress has been made in electrocatalyst modifications and system designs for high selectivity electro-oxidation towards valuable chemicals. This review provides an overview of the introduction of fuel-cell setup and potential reaction routes, as well as summaries of the products, performance, and system designs. Although this technology is promising, further research may concentrate on, but not be limited to the followings: (1) ascertain the reaction pathways of alcohol electro-oxidation on various electrocatalysts; (2) synthesize high selectivity, high durability, and non-precious electrocatalysts for alcohol electro-oxidation; (3) develop novel system designs for high mass transport and low cost; and (4) expand the utilization in a wider extent of toxic ions in industrial wastewater.

Acknowledgements

The work described in this paper was fully supported by a grant from the Natural Science Foundation of China (Project No. 51506039).

References

[1] J. Cheng, G.H. He, F.X. Zhang, A mini-review on anion exchange membranes for

fuel cell applications: Stability issue and addressing strategies, *Int. J. Hydrogen Energy* 40 (2015) 7348-7360.

[2] L. An, T.S. Zhao, An alkaline direct ethanol fuel cell with a cation exchange membrane, *Energy Environ. Sci.* 4 (2011) 2213-2217.

[3] J.R. Varcoe, P. Atanassov, D.R. Dekel, A.M. Herring, M.A. Hickner, P.A. Kohl, A.R. Kucernak, W.E. Mustain, K. Nijmeijer, K. Scott, T.W. X, L. Zhuang, Anion-exchange membranes in electrochemical energy systems, *Energy Environ. Sci.* 7 (2014) 3135-3191.

[4] L. An, T.S. Zhao, Y.S. Li, Q.X. Wu, Charge carriers in alkaline direct oxidation fuel cells, *Energy Environ. Sci.* 5 (2012) 7536-7538.

[5] R. Zeng, J. Handsel, S.D. Poynton, A.J. Roberts, R.C.T. Slade, H. Herman, D.C. Apperley, J.R. Varcoe, Alkaline ionomer with tuneable water uptakes for electrochemical energy technologies, *Energy Environ. Sci.* 4 (2011) 4925-4928.

[6] L. An, T.S. Zhao, R. Chen, Q.X. Wu, A novel direct ethanol fuel cell with high power density, *J. Power Sources* 196 (2011) 6219-6222.

[7] K. Jiao, P. He, Q. Du, Y. Yin, Three-dimensional multiphase modeling of alkaline anion exchange membrane fuel cell, *Int. J. Hydrogen Energy* 39 (2014) 5981-5995.

[8] L. An, T.S. Zhao, S.Y. Shen, Q.X. Wu, R. Chen, An alkaline direct oxidation fuel cell with non-platinum catalysts capable of converting glucose to electricity at high

power output, *J. Power Sources* 196 (2011) 186-190.

[9] K.H. Gopi, S.G. Peera, S.D. Bhat, P. Sridhar, S. Pitchumani, Preparation and characterization of quaternary ammonium functionalized poly(2,6-dimethyl-1,4-phenylene oxide) as anion exchange membrane for alkaline polymer electrolyte fuel cells, *Int. J. Hydrogen Energy* 39 (2014) 2659-2668.

[10] L. An, T.S. Zhao, Y.S. Li, Carbon-neutral sustainable energy technology: Direct ethanol fuel cells, *Renew. Sustain. Energy Rev.* 50 (2015) 1462-1468.

[11] Y.T. Luo, J.C. Guo, C.S. Wang, D. Chu, Fuel cell durability enhancement by crosslinking alkaline anion exchange membrane electrolyte, *Electrochemistry Communications* 16 (2012) 65-68.

[12] L. An, R. Chen, Direct formate fuel cells: A review, *J. Power Sources* 320 (2016) 127-139.

[13] A. Jasti, V.K. Shahi, Highly stable self-crosslinked anion conductive ionomers for fuel cell applications, *RSC Adv.* 4 (2014) 19238-19241.

[14] L. An, T.S. Zhao, X.H. Yan, X.L. Zhou, P. Tan, The dual role of hydrogen peroxide in fuel cells, *Science Bulletin* 60 (2015) 55-64.

[15] M.Z.F. Kamarudin, S.K. Kamarudin, M.S. Masdar, W.R.W. Daud, Review: Direct ethanol fuel cells, *Int. J. Hydrogen Energy* 40 (2015) 7348-7360.

[16] L. An, R. Chen, Recent progress in alkaline direct ethylene glycol fuel cells for

sustainable energy production, *J. Power Sources* 329 (2016) 484-501.

[17] Q.G. He, E.J. Cairns, Review-recent progress in electrocatalysts for oxygen reduction suitable for alkaline anion exchange membrane fuel cells, *J. The Electrochemical Society* 162 (2015) F1504-F1539.

[18] Z.C. Wang, L. Xin, X.S. Zhao, Y. Qiu, Z.Y. Zhang, O.A. Baturina, W.Z. Li, Carbon supported Ag nanoparticles with different particle size as cathode catalysts for anion exchange membrane direct glycerol fuel cells, *Renewable Energy* 62 (2014) 556-562.

[19] L. An, T.S. Zhao, Transport phenomena in alkaline direct ethanol fuel cells for sustainable energy production, *J. Power Sources* 341 (2017) 199-211.

[20] T. Fujigaya, C.R. Kim, K. Matsumoto, N. Nakashima, Palladium-based anion-exchange membrane fuel cell using KOH-doped polybenzimidazole as the electrolyte, *ChemPlusChem* 79 (2014) 400-405.

[21] D.W. Seo, Y.D. Lim, M.A. Hossain, S.H. Lee, H.C. Lee, H.H. Jang, S.Y. Choi, W.G. Kim, Anion conductive poly(tetraphenyl phthalazine ether sulfone) containing tetra quaternary ammonium hydroxide for alkaline fuel cell application, *Int. J. Hydrogen Energy* 38 (2013) 579-587.

[22] L. An, Z.H. Chai, L. Zeng, P. Tan, T.S. Zhao, Mathematical modeling of alkaline direct ethanol fuel cells, *Int. J. Hydrogen Energy* 38 (2013) 14067-14075.

- [23] J.R. Varcoe, M. Beillard, D.M. Halepoto, J.P. Kizewski, S.D. Poynton, R.C.T. Slade, Membrane and electrode materials for alkaline membrane fuel cells, *ECS Transactions* 16 (2008) 1819-1834.
- [24] L. An, T.S. Zhao, Z.H. Chai, L. Zeng, P. Tan, Modeling of the mixed potential in hydrogen peroxide-based fuel cells, *Int. J. Hydrogen Energy* 39 (2014) 7407-7416.
- [25] L. An, T.S. Zhao, Z.H. Chai, P. Tan, L. Zeng, Mathematical modeling of an anion-exchange membrane water electrolyzer for hydrogen production, *Int. J. Hydrogen Energy* 39 (2014) 19869-19876.
- [26] L. An, T.S. Zhao, X.L. Zhou, L. Wei, X.H. Yan, A high-performance ethanol-hydrogen peroxide fuel cell, *RSC Adv.* 4 (2014) 65031-65034.
- [27] L. An, T.S. Zhao, X.L. Zhou, X.H. Yan, C.Y. Jung, A low-cost, high-performance zinc-hydrogen peroxide fuel cell, *J. Power Sources* 275 (2015) 831-834.
- [28] F.J.R. Varela, S.F. Luna, O. Savadogo, Synthesis and evaluation of highly tolerant Pd electrocatalysts as cathodes in direct ethylene glycol fuel cells (DEGFC), *Energies* 2 (2009) 944-956.
- [29] L. An, T.S. Zhao, J.B. Xu, A bi-functional cathode structure for alkaline-acid direct ethanol fuel cells, *Int. J. Hydrogen Energy* 36 (2011) 13089-13095.
- [30] L. An, T.S. Zhao, L. Zeng, Agar chemical hydrogel electrode binder for fuel-electrolyte-fed fuel cells, *Applied Energy* 109 (2013) 67-71.

- [31] H.A. Miller, F. Vizza, A. Lavacchi, Nanomaterials for fuel cell catalysis, Springer, 2016 (Chapter 12).
- [32] W.R. Davis, J. Tomsho, S. Nikam, E.M. Cook, D. Somand, J.A. Peliska, Inhibition of HIV-1 reverse transcriptase-catalyzed DNA strand transfer reactions by 4-chlorophenylhydrazone of mesoxalic acid. *Biochemistry* 39 (2000) 14279-14291.
- [33] K. Kosaka, Y. Akanuma, Historical changes in diabetes therapy in Japan. *Diabetes Research and Clinical Practice* 24 (1994) S221-S227.
- [34] C.A. Gandolfi, L. Cotini, M. Mantovanini, G. Caselli, G. Clavenna, Omini C (Dompe Farmaceutici S.P.A). WO 1994010127 A1, 1994.
- [35] Powers T (Multisorb Technologies Inc., Thomas Powers). WO 2005040304, 2005.
- [36] Powers T (Multisorb Technologies Inc., Thomas Powers). WO 2006016916, 2006.
- [37] Solovyov SE (Multisorb Technologies Inc., Thomas Powers). WO 2007013978, 2007.
- [38] Bizot PM, Bailey BR, Hicks PD (Nalco Chemical Co.). WO 9816475, 1998.
- [39] D. Prasanna, V. Selvaraj, Development of non-covalent ternary polymer-CNT composite as a novel supporting material for electrooxidation of glycerol, *RSC Adv.* 5 (2015) 98822-98833.

- [40] J. Qi, N. Benipal, C.H. Liang, W.Z. Li, PdAg/CNT catalyzed alcohol oxidation reaction for high-performance anion exchange membrane direct alcohol fuel cell (alcohol = methanol, ethanol, ethylene glycol and glycerol), *Applied Catalysis B: Environmental* 199 (2016) 494-503.
- [41] A. Marchionni, M. Bevilacqua, C. Bianchini, Y.X. Chen, J. Filippi, P. Fornasiero, A. Lavacchi, H. Miller, L.Q. Wang, F. Vizza, Electrooxidation of ethylene glycol and glycerol on pd-(ni-zn)/c anodes in direct alcohol fuel cells, *ChemSusChem* 6 (2013) 518-528.
- [42] J. Qi, L. Xin, D.J. Chadderton, Y. Qiu, Y.B. Jiang, N. Benipal, C.H. Liang, W.Z. Li, Electrocatalytic selective oxidation of glycerol to tartronate on Au/Canode catalysts in anion exchange membrane fuel cells with electricity cogeneration, *Applied Catalysis B: Environmental* 154 (2014) 360-368.
- [43] L. Thia, M.S. Xie, Z.L. Liu, X.M. Ge, Y.Z. Lu, W.E. Fong, X. Wang, Copper-modified gold nanoparticles as highly selective catalysts for glycerol electro-oxidation in alkaline solution, *ChemCatChem* 8 (2016) 3272-3278.
- [44] C. Bianchini, P.K. Shen, Palladium-based electrocatalysts for alcohol oxidation in half cells and in direct alcohol fuel cells, *Chem. Rev.* 109 (2009) 4183-4206.
- [45] K. Matsuoka, Y. Iriyama, T. Abe, M. Matsuoka, Z. Ogumi, Electro-oxidation of methanol and ethylene glycol on platinum in alkaline solution: poisoning effects and

product analysis, *Electrochimica Acta* 51 (2005) 1085-1090.

[46] L. Demarconnay, S. Brimaud, C. Coutanceau, J.-M. Leger, Ethylene glycol electrooxidation in alkaline medium at multi-metallic Pt based catalysts, *J. Electroanalytical Chemistry* 601 (2007) 169-180.

[47] V. Bambagioni, C. Bianchini, A. Marchionni, J. Filippi, F. Vizza, J. Teddy, P. Serp, M. Zhiani, Pd and Pt–Ru anode electrocatalysts supported on multi-walled carbon nanotubes and their use in passive and active direct alcohol fuel cells with an anion-exchange membrane (alcohol=methanol, ethanol, glycerol), *J. Power Sources* 190 (2009) 241-251.

[48] A. Zalineeva, S. Baranton, C. Coutanceau, How do Bi-modified palladium nanoparticles work towards glycerol electrooxidation? An in situ FTIR study, *Electrochimica Acta* 176 (2015) 705-717.

[49] M. Simões, S. Baranton, C. Coutanceau, Enhancement of catalytic properties for glycerol electrooxidation on Pt and Pd nanoparticles induced by Bi surface modification, *Applied Catalysis B: Environmental* 110 (2011) 40-49.

[50] V.L. Oliveiraa, C. Morais, K. Servat, T.W. Napporn, G. Tremiliosi-Filho, K.B. Kokoh, Studies of the reaction products resulted from glycerol electrooxidation on Ni-based materials in alkaline medium, *Electrochimica Acta* 117 (2014) 255-262.

[51] T. Matsumoto, M. Sadakiyo, M.L. Ooi, S. Kitano, T. Yamamoto, S. Matsumura,

K. Kato, T. Takeguchi, M. Yamauchi, CO₂-free power generation on an iron group nanoalloy catalyst via selective oxidation of ethylene glycol to oxalic acid in alkaline media, *Scientific Reports* 4 (2014) 5620-5625.

[52] Z.Y. Zhang, L. Xin, J. Qi, Z.C. Wang, W.Z. Li, Selective electro-conversion of glycerol to glycolate on carbon nanotube supported gold catalyst, *Green Chem.* 14 (2012) 2150-2152.

[53] Z.Y. Zhang, L. Xin, W.Z. Li, Electrocatalytic oxidation of glycerol on Pt/C in anion-exchange membrane fuel cell: Cogeneration of electricity and valuable chemicals, *Applied Catalysis B: Environmental* 119 (2012) 40-48.

[54] H.B. Wang, L. Thia, N. Li, X.M. Ge, Z.L. Liu, X. Wang, Selective electro-oxidation of glycerol over Au supported on extendedpoly(4-vinylpyridine) functionalized graphene, *Applied Catalysis B: Environmental* 166 (2015) 25-31.

[55] A.K. Singh, S. Singh, A. Kumar, Hydrogen energy future with formic acid: a renewable chemical hydrogen storage system, *Catal. Sci. Technol.* (6) 2016 12-40.

[56] H.B. Wang, L. Thia, N. Li, X.M. Ge, Z.L. Liu, X. Wang, Pd nanoparticles on carbon nitride-graphene for the selective electro-oxidation of glycerol in alkaline solution, *ACS Catal.* 5 (2015) 3174-3180.

[57] N. Benipal, J. Qi, Q. Liu, W.Z. Li, Carbon nanotube supported PdAg nanoparticles for electrocatalytic oxidation of glycerol in anion exchange membrane

fuel cells, *Applied Catalysis B: Environmental* 210 (2017) 121-130.

[58] O.O. Fashedemi, H.A. Miller, A. Marchionni, F. Vizza, K.I. Ozoemena, Electro-oxidation of ethylene glycol and glycerol at palladium-decorated FeCo@Fe core-shell nanocatalysts for alkaline direct alcohol fuel cells: functionalized MWCNT supports and impact on product selectivity, *J. Mater. Chem. A* 3 (2015) 7145-7156.

[59] Z.Y. Zhang, L. Xin, J. Qi, D.J. Chadderdon, K. Sun, K.M. Warsko, W.Z. Li, Selective electro-oxidation of glycerol to tartronate or mesoxalate on Au nanoparticle catalyst via electrode potential tuning in anion-exchange membrane electro-catalytic flow reactor, *Applied Catalysis B: Environmental* 147 (2014) 871-878.

[60] M. Simoes, S. Baranton, C. Coutanceau, Electro-oxidation of glycerol at Pd based nano-catalysts for an application in alkaline fuel cells for chemicals and energy cogeneration, *Applied Catalysis B: Environmental* 93 (2010) 354-362.

[61] L. Xin, Z.Y. Zhang, Z.C. Wang, W.Z. Li, Simultaneous generation of mesoxalic acid and electricity from glycerol on a gold anode catalyst in anion-exchange membrane fuel cells, *ChemCatChem* 4 (2012) 1105-1114.

[62] D.J. Chadderdon, L. Xin, J. Qi, B. Brady, J.A. Miller, K. Sun, M.J. Janik, W.Z. Li, Selective oxidation of 1,2-propanediol in alkaline anion-exchange membrane electrocatalytic flow reactors: Experimental and DFT investigations, *ACS Catal.* 5 (2015) 6926-6936.

- [63] L.M. Palma, T.S. Almeida, C. Morais, T.W. Napporn, K.B. Kokoh, A.R.D. Andrade, Effect of the Co-catalyst on the selective electrooxidation of glycerol over ruthenium based nanomaterials, *ChemElectroChem* 4 (2017) 39-45.
- [64] Y.S. Li, Y. Feng, X.D. Sun, Y.L. He, A sodium-ion-conducting direct formate fuel cell: generating electricity and producing base, *Angew. Chem. Int. Ed.* 129 (2017) 5828-5831.
- [65] J. González-Cobos, S. Baranton, C. Coutanceau, A systematic in situ infrared study of the electrooxidation of C3 alcohols on carbon-supported Pt and Pt-Bi catalysts, *J. Phys. Chem. C* 120 (2016) 7155-7164.
- [66] J. González-Cobos, S. Baranton, C. Coutanceau, Development of Bi-modified ptpd nanocatalysts for the electrochemical reforming of polyols into hydrogen and value-added chemicals, *ChemElectroChem* 3 (2016) 1694-1704.
- [67] L. Xin, Z.Y. Zhang, J. Qi, D.J. Chadderdon, Y. Qiu, K.M. Warsko, W.Z. Li, Electricity storage in biofuels: selective electrocatalytic reduction of levulinic acid to valeric acid or γ -valerolactone, *ChemSusChem* 6 (2013) 674-686.
- [68] B. Wouters, J. Hereijgers, W.D. Malsche, T. Breugelmans, A. Hubin, Electrochemical characterisation of a microfluidic reactor for cogeneration of chemicals and electricity, *Electrochimica Acta* 210 (2016) 337-345.
- [69] M.A. Goulet, E. Kjeang, Co-laminar flow cells for electrochemical energy

conversion, *J. Power Sources* 260 (2014) 186-196.

[70] J. Xuan, M.K. Leung, D.Y. Leung, M. Ni, H. Wang, Hydrodynamic focusing in microfluidic membraneless fuel cells: Breaking the trade-off between fuel utilization and current density, *Int. J. Hydrogen Energy*. 36 (2011) 11075-11084.

[71] E. Kjeang, N. Djilali, D. Sinton, Microfluidic fuel cells: A review, *J. Power Sources* 186 (2009) 353-369.

[72] A.S. Knight, E.Y. Zhou, J.G. Pelton, M.B. Francis, Selective chromium(VI) ligands identified using combinatorial peptoid libraries, *J. Am. Chem. Soc.* 135 (2013) 17488-17493.

[73] B.R. James, The challenge of remediating chromium-contaminated soil, *Environ. Sci. Technol.* 30 (1996) A248-A251.

[74] Y.L. Zhang, Y.M. Li, J.F. Li, G.D. Sheng, Y. Zhang, X.M. Zheng, Enhanced Cr(VI) removal by using the mixture of pillared bentonite and zero-valent iron, *Chem. Eng. J.* 185 (2012) 243-249.

[75] H.M. Zhang, W. Xu, Z.C. Wu, M.H. Zhou, T. Jin, Removal of Cr(VI) with cogeneration of electricity by an alkaline fuel cell reactor, *J. Phys. Chem. C* 117 (2013) 14479-14484.

[76] W. Xu, H.M. Zhang, G. Li, Z.C. Wu, A urine/Cr(VI) fuel cell - Electrical power from processing heavy metal and human urine, *J. Electroanalytical Chemistry* 764

(2016) 38-44.

[77] H.M. Zhang, W. Xu, Z. Fan, X. Liu, Z.C. Wu, M.H. Zhou, Simultaneous removal of phenol and dichromate from aqueous solution through a phenol-Cr(VI) coupled redox fuel cell reactor, *Separation and Purification Technology* 172 (2017) 152-157.

Table caption:

Table 1 Selected conversion performance reported in the open literature.

Figure captions:

Figure 1 Schematic of a typical alkaline anion exchange membrane fuel cell (AAEMFC).

Figure 2 (a) Proposed mechanism for ethylene glycol electro-oxidation [44].

Reproduced with permission from American Chemical Society. (b) (c) (d) (e)

Proposed mechanism for glycerol electro-oxidation [47] [48] [49]. Reproduced with permission from Elsevier.

Figure 3 (a) The product selectivity of Pd NPs on different supports (CB, CN_x,

CN_x/G) at various potentials. (b) The mechanistic of glycerol oxidation [56].

Reproduced with permission from American Chemical Society.

Figure 4 Scheme of the preparation of a FeCoNi nanoalloy catalyst loaded on carbon

[51]. Reproduced with permission from Nature Publishing.

Figure 5 (a) The product selectivity of glycerol electro-oxidation on Au/CNT at

various potentials [52]. Reproduced with permission from The Royal Society of

Chemistry. (b) The product selectivity of glycerol electro-oxidation on Au/C at

various potentials [59]. Reproduced with permission from Elsevier.

Figure 6 (a) Product selectivity during glycerol electro-oxidation over catalysts

prepared at +0.015 V for different durations. Formate=, glycolate=, oxalate=, glycerate=, tartronate= [43]. Reproduced with permission from Wiley. (b) The product selectivity of PDO electrooxidation on (i) Pt/C and (ii) Au/C at various potentials [62]. Reproduced with permission from American Chemical Society.

Figure 7 (a) Schematic of a single electrocatalytic (flow) cell reactor [67]. Reproduced with permission from Wiley. (b) Schematic of the anion exchange membrane-based electrocatalytic flow reactors [59]. Reproduced with permission from Elsevier.

Figure 8 (a) Schematic of a typical laminar flow fuel cell [68]. (b) Schematic of a typical urine/Cr(VI) fuel cell [76]. Reproduced with permission from Elsevier.